Wind tunnel investigation of the wake-flow response for a floating turbine subjected to surge motion

Wind tunnel investigation of the wake-flow response for a floating turbine subjected to surge motion

A. Fontanella[1], **A. Zasso**[1], **M. Belloli**[1]

[1] Mechanical Engineering Department, Politecnico di Milano, Milano, Via La Masa 1, 20156, Italy.

E-mail: alessandro.fontanella@polimi.it

Abstract. Floating wind turbines undergo large translation motions allowed by the high compliancy of the support structure. Large motions affect the rotor aerodynamic response and wake. This paper examines wake measurements of a wind tunnel experiment with a scale model of the DTU 10MW subjected to imposed harmonic surge motion. The effect of surge motion on the wake is detected by means of spectral analysis of velocity data. It is found that when the rotor undergoes surge motion, periodic forcing is introduced into the fluid, which produces a harmonic variation of the wake speed. The velocity perturbation around the rotor is then convected downstream at about the average axial velocity in the wake. The amplitude of the velocity pulsation at $2.3D$ is radially-dependent, and is correlated to the amplitude of the variation of the normal-force distribution along the blade.

1. Introduction

While the first commercial-scale floating turbines are becoming operational, the coupling between rotor aerodynamics and platform motion is far from being completely understood. Floating turbines experience large motions during normal operation that can affect the aerodynamic response of rotor and wake. Wake interaction and the effects it has on the turbine global response for a two-turbine floating farm is studied in [1, 2] with FAST.Farm [3]. In [4] the case of two tandem floating turbines is analyzed using an actuator disk model.

In order to better estimate the power output and fatigue life of a floating farm, knowledge about the development and stability of wakes is crucial. Moreover, improved understanding of how the wake physics is affected by the large motions permitted by a floating foundation is key for validating turbine/wake models, it can guide the selection of metrics for numerical vs experimental comparison. In recent years wind tunnel experiments became central in the research about wakes and wind farm control for bottom fixed turbines for the possibility to generate low-uncertainty data in controlled environmental conditions, and perform measurements that are not feasible full-scale [5]. Few are the experiments about wakes in floating turbines. Research with actuator disc models was conducted to study the far-wake and the interaction with atmospheric wind. In [6] measurements of a porous-disk model subjected to pitch and roll oscillations show that turbine motion introduces some harmonic content in the wake velocity, which strength is proportional to motion amplitude. Also the far-wake measurements with a porous disk subjected to imposed surge motion of [7] show the wake energy content is increased at the motion frequency, with consequences for wake turbulence and recovery. Measurements with a scaled turbine makes it possible to study the physics of the

wake. Wind tunnel tests with a scale model of the DTU 10MW under imposed surge motion and laminar wind were conducted in [8, 9, 10], where it is found the wake spectral content is increased at the frequency of motion, that this effect is not the same for different radial positions, and is related to the amplitude/frequency of motion. In addition, the tip-vortex is studied with PIV and it is seen that, with surge motion, this is convected in the wake with a different speed than when the turbine is fixed.

The aim of this work is to provide more knowledge on the wake-flow response for a floating turbine subjected to surge motion, by further analyzing the hot-wire and PIV measurements of the full-turbine experiments of [10] (the dataset is freely available at [11]). Surge motion is in the along wind direction and causes an apparent wind for the rotor, which results into a pulsating thrust force. The main outcome of this research is that the pulsating wake velocity caused by surge motion is correlated to the aerodynamic response of the blade and to the wake convection process.

2. Methodology

This section describes the wind tunnel experiment setup and the test matrix.

2.1. Test setup

Testing was conducted in the boundary layer test section of the Politecnico di Milano wind tunnel, which is a closed-return facility with a cross section 13.84 m wide $\times$ 3.84 m high. The wind turbine is a 1/75 model of the DTU 10MW with a rotor diameter of 2.38 m. The turbine rotor uses low-Reynolds airfoils and the blade chord and twist were selected to preserve the distribution of lift force despite of the reduced Reynolds number in the wind tunnel, as explained in detail in [12]. The axial speed deficit in the wake is largely set by the rotor normal force (and lift force), thus the scaling approach allows to consider the wake of the model as representative that of a full-size turbine [5].

The test setup is shown in Fig. 1. The turbine tower is mounted on top of a robot that moves it in the along wind direction, and is tilted of 5° upwind to offset the rotor tilt and have the rotor normal to ground. The free-stream wind speed was measured at hub-height 7.15 m upstream the rotor with a pitot tube. The turbine far wake was measured with hot-wire probes at a downstream distance of $2.3D$ and hub-height, spanning the wake width in between $z = \pm 1.3R$ in steps of $0.08R$. The wake was measured along the axial direction in between $x = 0.9$–$2.3D$ in steps of $0.14D$, at hub-height and $z = 0.75R$. Wake measurements were carried out without and with surge motion. The near-wake was scanned with particle image velocimetry (PIV). The measurement window is aligned with the rotor centerline, and spans $x = 0.25$–$0.55D$, $y = 0.5$–$1.3R$. Also PIV measurements were conducted without and with imposed motion. In the first case, PIV images were phase-locked to the rotor azimuth position, in the second to the the turbine position in the surge cycle.

2.2. Test matrix

The experiment considered two turbine operating conditions, with a wind velocity of 4 m/s (rated) and 6 m/s (above-rated). The turbine was run with fixed rotor speed and blade-pitch angle, that were set to the values reported in Tab. 1. All tests were done with laminar wind (turbulence intensity around 2%). Measurements were carried out without imposed motion to set the reference condition for tests with motion, in which the turbine was forced to moved in surge. Surge motion is mono-harmonic, of different frequencies and amplitudes, that were selected to avoid dynamic stall (see [10]) and to be representative of multi-megawatt floating turbines. Floating turbines of 10 MW rating have the surge mode natural frequency in a range of 0.01–0.03 Hz [2, 13] which corresponds to 0.25–0.75 Hz at model scale. Among all cases run in the experimental campaign, the subset reported in Tab. 1 is considered for the present analyses.

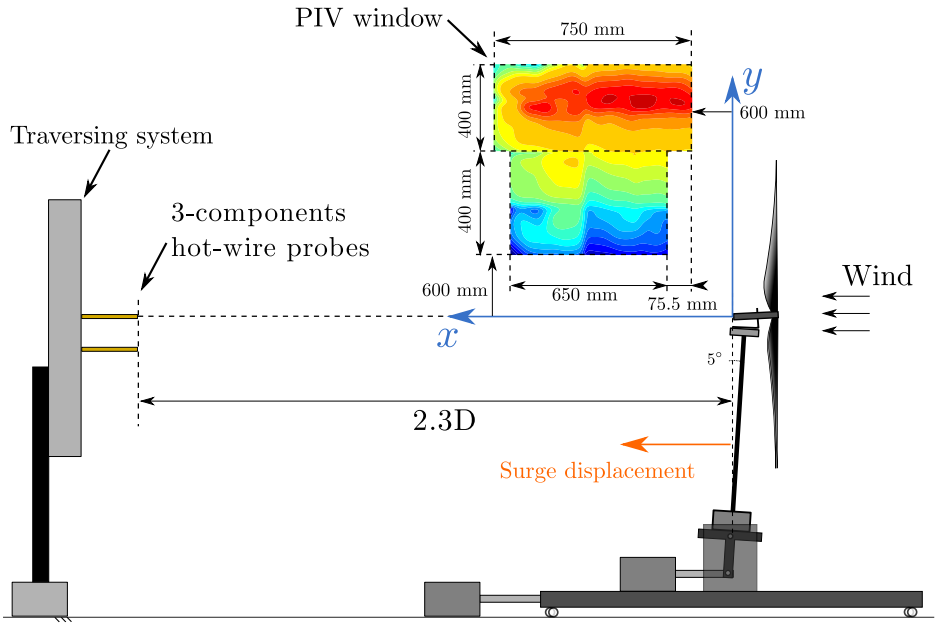

Figure 1. Scheme of the test setup in the PoliMi wind tunnel and conventions of sign for results.

Table 1. Turbine and motion conditions analyzed in the experiment.

Condition	TN	Wind speed [m/s]	Rotor speed [rpm]	Blade pitch [deg]	Steady $C_{t,0}$ [−]	Surge frequency [Hz]	Surge amplitude [m]	Surge $\Delta V/V$ [−]
Rated	1	4.0	240	0.0	0.87	–	–	–
Rated	2	4.0	240	0.0	0.87	0.125	0.125	0.02
Rated	3	4.0	240	0.0	0.87	0.500	0.065	0.05
Rated	4	4.0	240	0.0	0.87	1.000	0.035	0.05
Above	5	6.0	265	12.5	0.19	–	–	–
Above	6	6.0	265	12.5	0.19	0.125	0.125	0.02
Above	7	6.0	265	12.5	0.19	1.000	0.050	0.05

3. Results

This section describes the results of measurements. Focus of the analysis is the axial velocity in the wake and how this is modified when the turbine moves in surge. From a wind farm perspective, the axial velocity determines the inflow condition for downstream turbines. In Sect. 3.1 the average wake deficit is examined to see if wake recovery is affected by platform motion. Then, Sect. 3.2 and 3.3 study the velocity pulsation at the frequency of imposed motion in the far- and near-wake. Sect. 3.4 and 3.4 correlate the magnitude and phase of the velocity oscillations to the normal force distribution along the blade and to the convection velocity.

3.1. Average wake deficit

Figure 2 shows the average speed deficit for all test cases of Tab. 1 that was measured at 2.3D and normalized by the free-stream velocity U_∞. The wake deficit exhibits a double-gaussian profile for cases with $U_\infty = 4$ m/s, and gaussian for $U_\infty = 6$ m/s. In both conditions it is slightly asymmetric with respect to the wake centerline, and velocity is lower for negative radial positions. Asymmetry is likely an effect of anisotropic blockage: the wind tunnel section is large compared to rotor ($A_{\text{rotor}}/A_{\text{tunnel}} = 0.08$) but the height is comparable to rotor diameter ($D/h_{\text{tunnel}} = 0.62$). With imposed motion, the wake deficit is about the same than with fixed turbine so, in the investigated conditions, there is no evidence of increased mean-velocity recovery.

3.2. Far-wake response to imposed motion

The effect of surge motion on the wake is detected by means of spectral analysis of hot-wire data. Having computed the FRF of the axial velocity at r_i/R, the harmonic component at the surge frequency is taken and reported in terms of amplitude and phase in Fig. 3. This represents the harmonic fluctuation of the axial velocity caused by the imposed motion of the rotor. The amplitude of wake oscillations never exceeds 4% of the free-stream speed, is proportional to, but lower than, the apparent wind speed due to surge $\Delta V/V$. Phase is equal for tests with the same free-stream speed, and it is about $-\pi/4$ for cases with $U_\infty = 4$ m/s, $-3\pi/4$ for those with $U_\infty = 6$ m/s. Velocity oscillations show a marked dependence on the radial position. The trend is consistent for all cases with the same U_∞, and so the same turbine operating condition. As for the average deficit, velocity oscillations are not symmetric about the rotor centerline. Phase-data across the wake for TN2 are more dispersed than in any other case.

3.3. Near-wake response to imposed motion

PIV is utilized to investigate the velocity field behind the rotor and how its structure is modified in presence of surge motion. The reference condition is set by the average axial flow-field in the fixed-turbine case, which is obtained by the ensemble-average of PIV images for different rotor-azimuth angles (from $\psi = 0°$ to $\psi = 120°$ every 15° and from $\psi = 120°$ to $\psi = 360°$ every 30°, 100 images for every angle). For cases with surge motion, the flow field is obtained by the

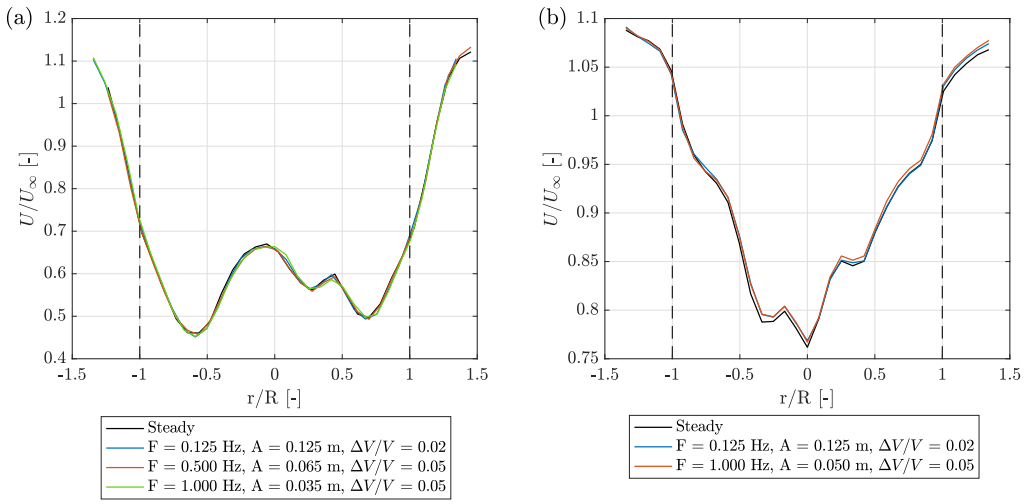

Figure 2. Average wake deficit at 2.3D, hub height. **(a)** rated ($U_\infty = 4$ m/s), **(b)** above-rated ($U_\infty = 6$ m/s). The vertical dashed lines mark the edge of the rotor.

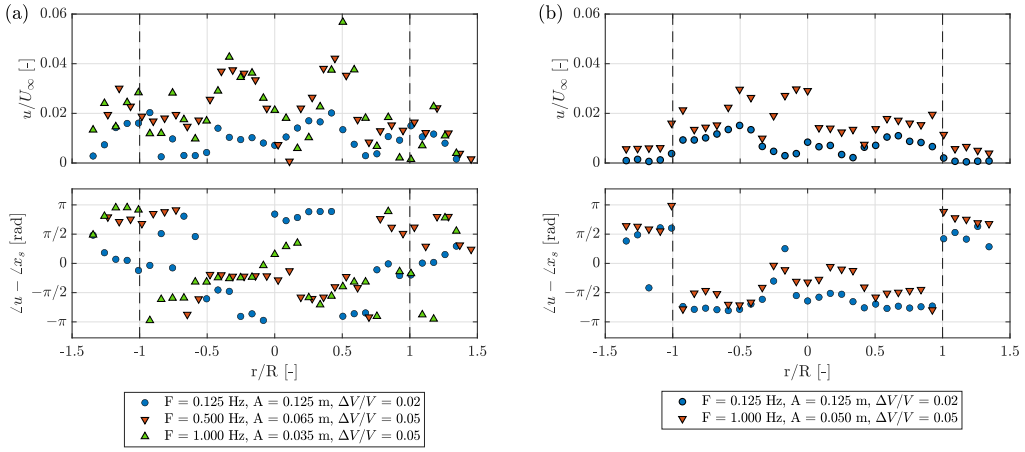

Figure 3. Amplitude (top) and phase with respect to surge (bottom) of the axial velocity spectral component with frequency equal to the surge motion frequency. **(a)** rated ($U_\infty = 4$ m/s), **(b)** above-rated ($U_\infty = 6$ m/s). The vertical dashed lines mark the edge of the rotor.

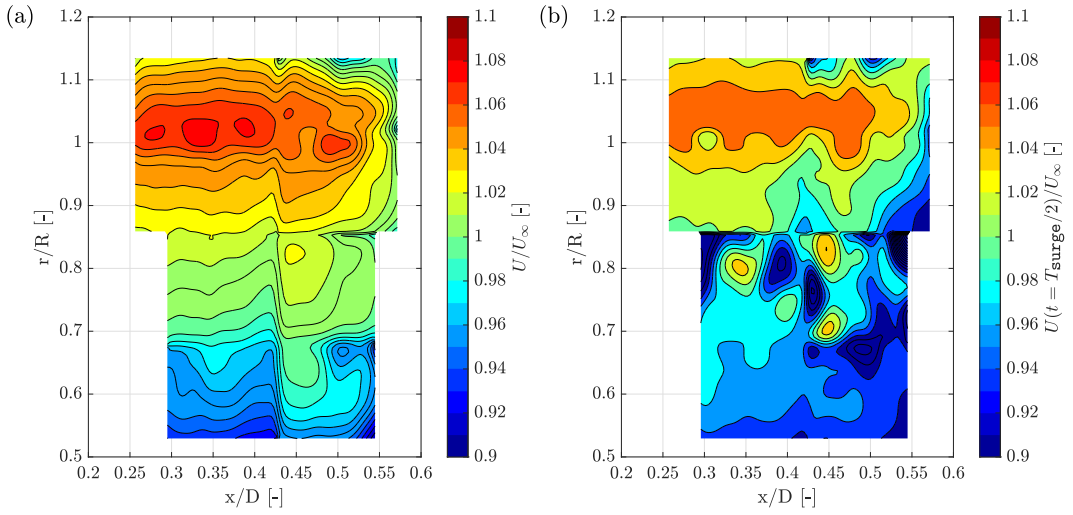

Figure 4. Contour map of the velocity deficit field behind the turbine rotor. **(a)** with no motion, **(b)** with surge motion ($U_\infty = 6$ m/s, $F = 1$ Hz, $A = 0.05$ m) at half surge period, i.e. with the turbine passing for the zero-surge position moving upwind.

phase-average of images taken at evenly spaced positions in the surge oscillation, regardless of rotor azimuth.

The velocity deficit with no motion and with motion for TN7, the above-rated case with the largest ΔV, is shown in Fig. 4. The structure of the innermost region of the wake is significantly altered when the turbine is forced to move. In the region $r/R = 0.5$–0.9 the gradually-decreasing velocity of the steady case (a), is replaced in (b) by local peaks alternated to troughs, particularly evident in the region ($r/R = 0.75$–0.85, $x/D = 0.3$–0.55). The region about the rotor edge ($r/R = 1$) is characterized by a slight overspeed, which can be reasonably attributed to blockage caused by the close proximity with ceiling. With surge, the overspeed region is confined to a smaller area, but there are no evident peak-troughs as in the core of the wake.

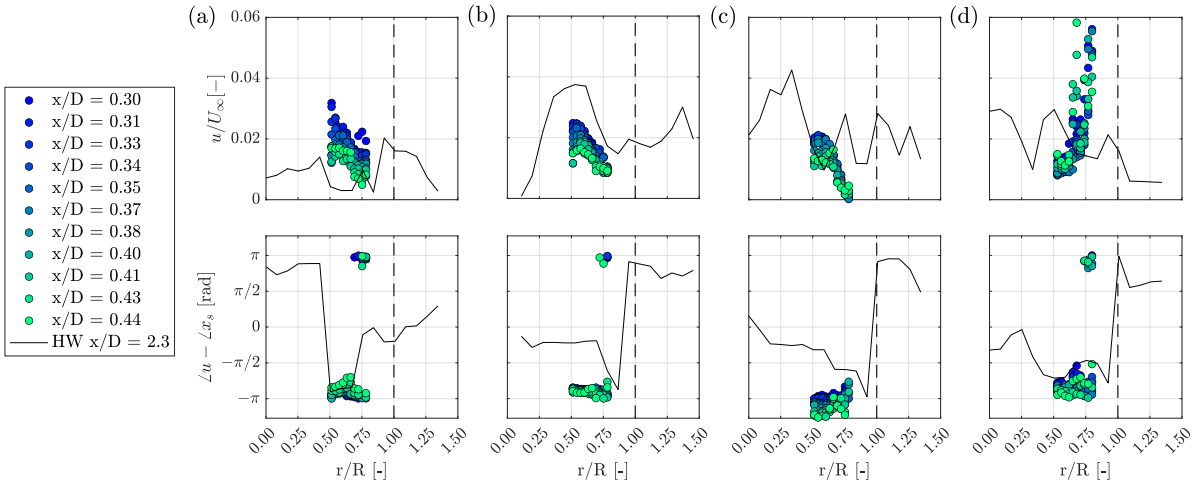

Figure 5. Amplitude (top) and phase with respect to surge (bottom) of the axial velocity spectral component with frequency equal to the surge motion frequency. **(a)**: TN2, **(b)**: TN3, **(c)**: TN4, **(d)**: TN7. Far-wake results of Fig. 3 are reported for reference as "HW x/D = 2.3". The vertical dashed lines mark the edge of the rotor.

The effect of imposed surge motion on the near-wake flow in the plane x–y is detected by means of spectral analysis, similarly to what is done in Sect. 3.2 for far-wake measurements in the x–z plane. The magnitude and phase of the surge-frequency harmonic of the axial velocity is shown in Fig. 5 for different radial positions r/R and variable downwind distance x/D. Compared to far-wake results of Fig. 3, the amplitude of velocity fluctuations is generally lower for cases TN3, TN4 (rated), and higher for TN2 (rated) and TN7 (above-rated). The amplitude decreases moving downstream the near-wake region, i.e., for increasing x/D. Phase is about $-\pi$ for radial locations $r/R = 0.5$–0.75, and is different than at $x = 2.3D$.

3.4. Amplitude of wake-velocity oscillations and blade normal force

To explain the radial dependence of the amplitude of velocity variation, far-wake results of Fig. 3 are compared to the normal force along the blade. The normal force F_N is shown on the left of Fig. 6. When the turbine is moved in surge, the rotor experiences a variable inflow velocity, that also produces a variation of the angle of attack along the blade. The combination of these effects gives a pulsating normal force, which peak-to-peak range $\pm\Delta F_N$ is shown for two motion conditions by the shaded area. The right of Fig. 6 correlates the amplitude of the normal force oscillation ΔF_N to the amplitude of wake oscillations with nice agreement. The process by which the forced surge motion is translated into the pulsing wake velocity is resumed in the schematic of Fig. 7.

3.5. Phase of wake-velocity oscillations and convection speed

The pulsating thrust force due to imposed surge motion introduces a periodic forcing into the fluid, which produces a periodic variation of the wake speed. The velocity perturbation around the rotor is then convected downstream. The propagation of the velocity perturbation is examined looking at the spectrum of the axial velocity along the wake at 0.75R. In particular, by looking at the amplitude and phase-shift of the spectral component with frequency equal to the surge motion frequency, which is shown in Fig. 8 for TN3, TN4 and TN7. Amplitude is increased passing from the near-wake to the far-wake, due to the speed recovery that takes place. Phase-shift is linearly-increasing with distance from rotor, and this witnesses that the

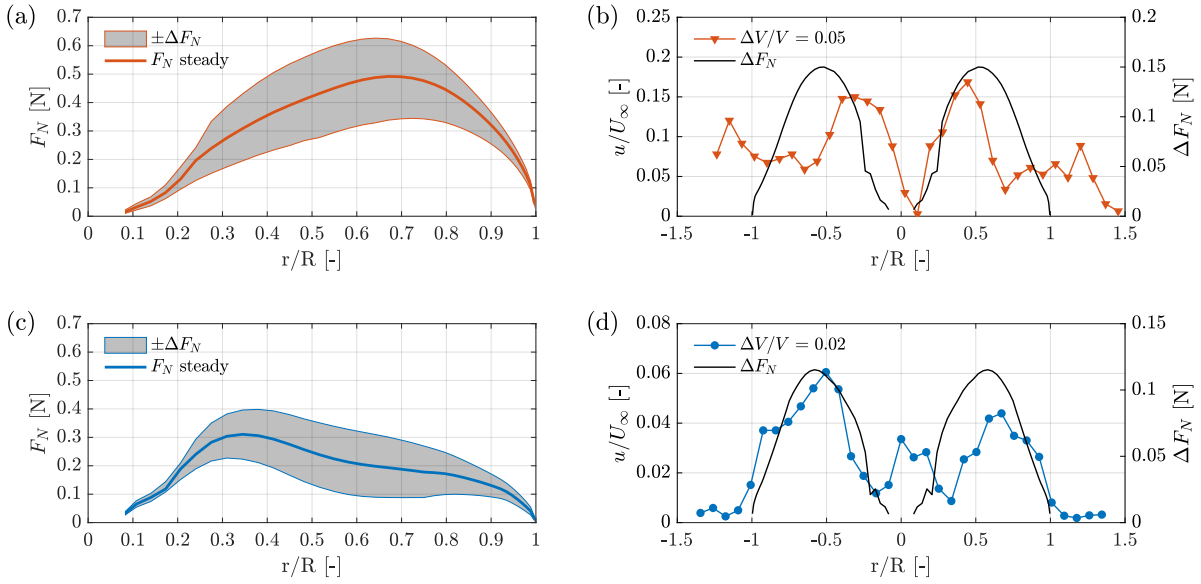

Figure 6. (a,c) normal force F_N along the blade span and variation with surge motion ΔF_N. **(b,d)** the variation of normal force is compared with the amplitude of the axial velocity spectral component at the surge frequency measured at 2.3D (as in Fig. 3). **(a,b)**: TN5 **(c,d)**: TN6.

velocity perturbation travels downstream at finite speed. The phase of velocity oscillations at a given location in the wake depends of the travel speed, and on the distance from rotor. This explain the difference in the phase observed in Fig. 6 between the near- and far-wake.

The travel speed u_{conv} is estimated from along-wind hot-wire data and PIV data of Fig. 8, by computing first the time it takes the velocity pulsation to travel from one location x_1 to a downstream one x_i:

$$\tau(x_i) = -\frac{\phi(x_i) - \phi(x_1)}{2\pi f_{\text{surge}}}\,. \tag{1}$$

The speed at which the speed perturbation travels from x_1 to x_i is:

$$u_{\text{conv}}(x_i) = \frac{x_i - x_1}{\tau(x_i)}\,. \tag{2}$$

Results for two rated conditions TN3 and TN4, and for one above-rated condition TN7 are reported in Fig. 9. Results from PIV data are the average of all the available x_i positions. Between 0.25–0.5D the velocity pulsation convects at about the theoretical velocity in the rotor plane, and 20% faster for TN4. After 1D the travel speed is lower, close to the theoretical velocity in the far wake, and 15% higher for TN4.

4. Conclusions

In this paper wind tunnel data about a wind turbine model subjected to imposed surge motion are used to gain additional knowledge about wake of floating turbines. The average axial-speed deficit at 2.3D is the same for the fixed turbine and with platform motion, so there is no clear evidence of improved wake recovery for the case at hand. The effect of surge motion on the wake is detected by means of spectral analysis of velocity data, and it is seen it mainly consists of oscillations of the axial speed with the same frequency of the imposed motion. The harmonic thrust force due to surge motion introduces a periodic forcing into the fluid, which produces

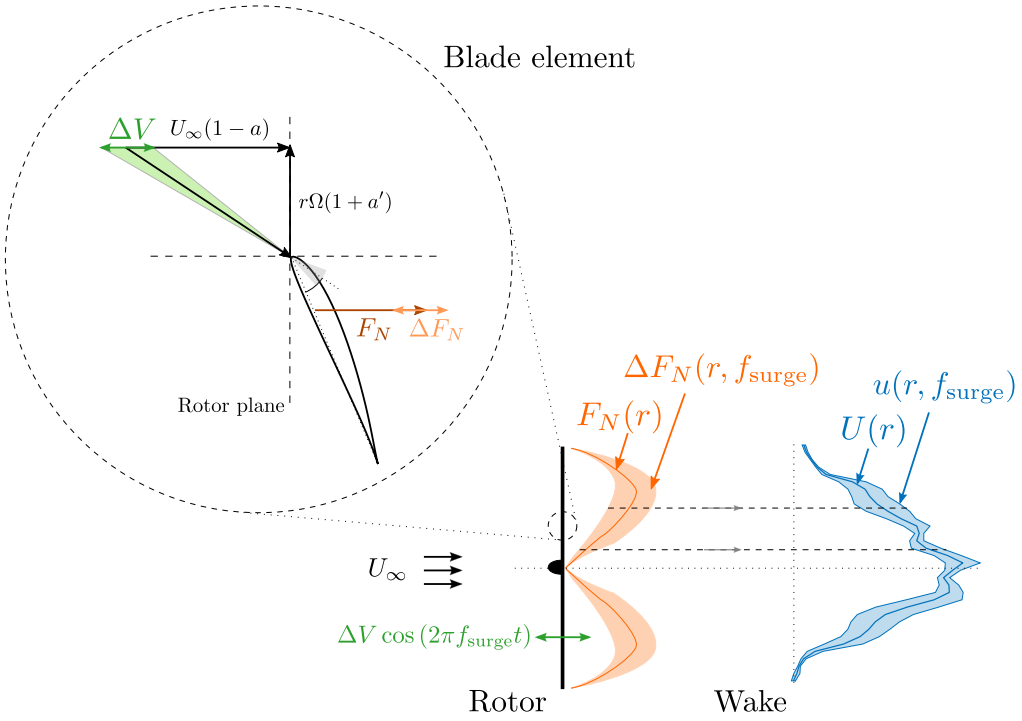

Figure 7. Mechanism by which the forced surge motion is translated into the pulsing wake velocity. The axial inflow speed of every element of the blade has a component of amplitude ΔV caused by surge motion. This results into a variable normal force which amplitude ΔF_N depends on the steady angle of attack, function of the blade element radial position r. The pulsating normal force at r directly translates into variations of the wake velocity of amplitude $u(r)$ which are superposed to the average speed $U(r)$.

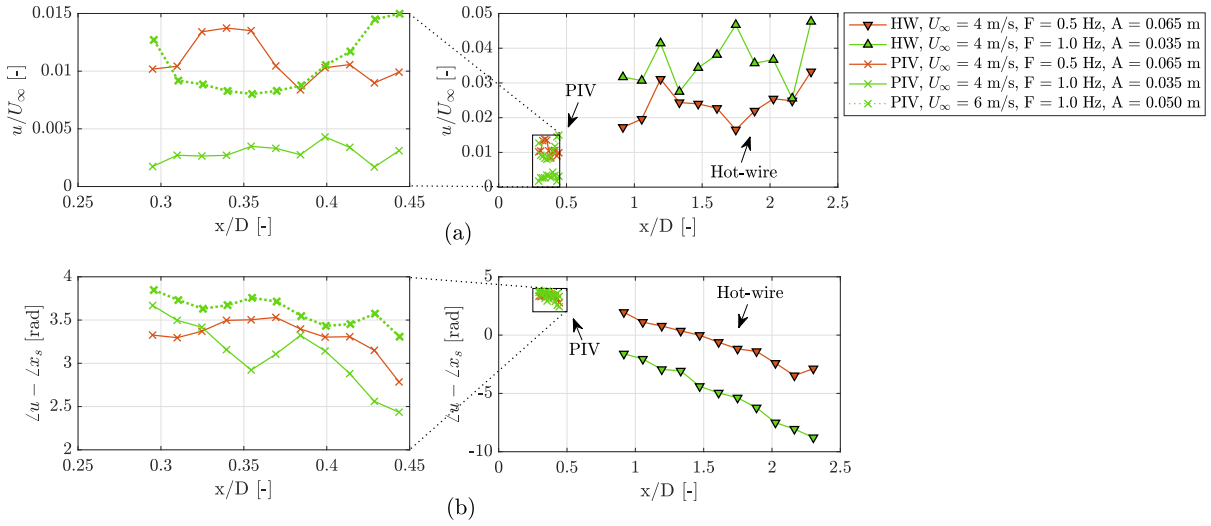

Figure 8. Spectra of the axial velocity along the wake from hot-wires (horizontal plane) and PIV (vertical plane) at $0.75R$. **(a)** amplitude, **(b)** phase with respect to imposed motion.

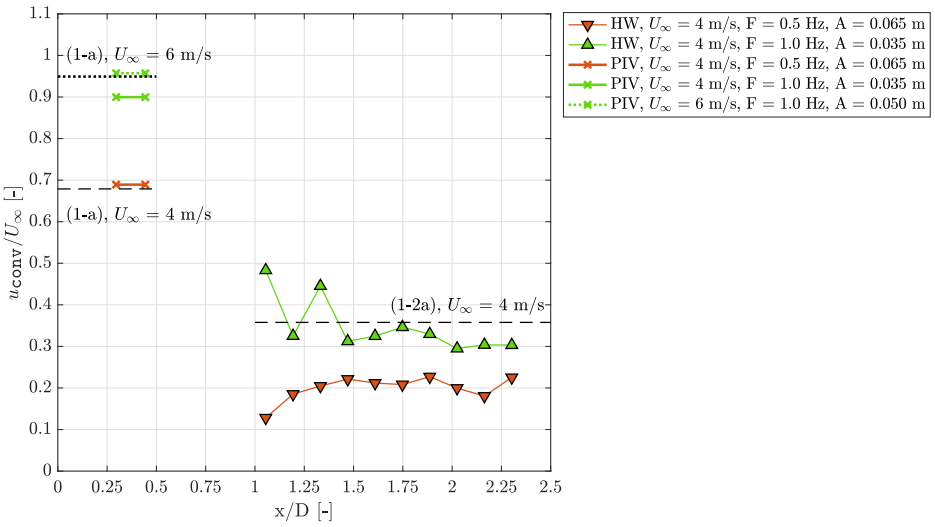

Figure 9. Convection speed of the surge-frequency velocity fluctuations normalized by free-stream velocity. $(1-a)$ and $(1-2a)$ are the theoretical velocity in the rotor plane and in the far wake, calculated based on the steady thrust coefficient reported in Tab. 1.

a periodic variation of the wake speed that is convected downstream at about the theoretical velocity in the wake. The amplitude of wake-velocity oscillations is not constant but depends on the radial position and it is correlated to the normal force distribution along the blade.

Here, wind tunnel data were analyzed to gain insight in the wake physics, but another way to use scale model data is for codes validation. Then, validated codes can be leveraged to study conditions which are not feasible to investigate with experiments. Validation of codes against the wake data discussed here is currently ongoing in the OC6 Phase III project.

Further investigation of the wake of floating turbines is advisable. Future experiments should measure the wake at greater downwind distances, and with platform motions other than surge. Pitch and yaw may affect the wake meandering with potential implications for the development of wake steering control strategies for floating farms.

5. Acknowledgements

The wind tunnel test campaing has been supported by EU-EERA (European Energy Research Alliance)/IRPWIND Joint Experiment 2017. The methodology for the analysis of wake data has been developed within the Horizon 2020 project COREWIND (grant no. 815083).

References

[1] A. Wise and E. E. Bachynski. Analysis of wake effects on global responses for a floating two-turbine case. *Journal of Physics: Conference Series*, 1356(1):012004, oct 2019.

[2] A. S. Wise and E. E. Bachynski. Wake meandering effects on floating wind turbines. *Wind Energy*, 23(5):1266–1285, 2020.

[3] J. M. Jonkman, J. Annoni, G. Hayman, B. Jonkman, and A. Purkayastha. *Development of FAST.Farm: A New Multi-Physics Engineering Tool for Wind-Farm Design and Analysis.*

[4] A. Rezaeiha and D. Micallef. Wake interactions of two tandem floating offshore wind turbines: Cfd analysis using actuator disc model. *Renewable Energy*, 179:859–876, 2021.

[5] C. Wang, F. Campagnolo, H. Canet, D. J. Barreiro, and C. L. Bottasso. How realistic are the wakes of scaled wind turbine models? *Wind Energy Science*, 6(3):961–981, 2021.

[6] S. Fu, Y. Jin, Y. Zheng, and L. P. Chamorro. Wake and power fluctuations of a model wind turbine subjected to pitch and roll oscillations. *Applied Energy*, 253:113605, 2019.

[7] Benyamin Schliffke, Sandrine Aubrun, and Boris Conan. Wind tunnel study of a "floating" wind turbine's wake in an atmospheric boundary layer with imposed characteristic surge motion. *Journal of Physics: Conference Series*, 1618:062015, sep 2020.

[8] I. Bayati, M. Belloli, L. Bernini, and A. Zasso. Wind tunnel wake measurements of floating offshore wind turbines. *Energy Procedia*, 137:214–222, 2017. 14th Deep Sea Offshore Wind R&D Conference, EERA DeepWind'2017.

[9] I. Bayati, L. Bernini, A. Zanotti, M. Belloli, and A. Zasso. Experimental investigation of the unsteady aerodynamics of FOWT through PIV and hot-wire wake measurements. *Journal of Physics: Conference Series*, 1037:052024, jun 2018.

[10] A. Fontanella, I. Bayati, R. Mikkelsen, M. Belloli, and A. Zasso. Unaflow: a holistic wind tunnel experiment about the aerodynamic response of floating wind turbines under imposed surge motion. *Wind Energy Science*, 6(5):1169–1190, 2021.

[11] A. Fontanella, I. Bayati, R. Mikkelsen, M. Belloli, and A. Zasso. UNAFLOW: UNsteady Aerodynamics of FLOating Wind turbines, May 2021. https://doi.org/10.5281/zenodo.4740006.

[12] I. Bayati, I. Belloli, L. Bernini, and A. Zasso. Aerodynamic design methodology for wind tunnel tests of wind turbine rotors. *Journal of Wind Engineering and Industrial Aerodynamics*, 167:217–227, 2017.

[13] J. Azcona, F. Vittori, U.S. Paulsen, F. Savenije, G. Kapogiannis, X. Karvelas, D. Manolas, S. Voutsinas, F. Amann, R. Faerron Guzman, and F. Lemmer. Design Solutions for 10MW Floating Offshore Wind Turbines. Deliverable 4.37. INNWIND.EU, 2017.